

PHYSICAL REVIEW D

PARTICLES AND FIELDS

THIRD SERIES, VOLUME 25, NUMBER 3

1 FEBRUARY 1982

Total cross sections for $\nu_\mu n$ and $\nu_\mu p$ charged-current interactions in the 7-foot bubble chamber

N. J. Baker, P. L. Connolly, S. A. Kahn, M. J. Murtagh,
R. B. Palmer, N. P. Samios, and M. Tanaka
Brookhaven National Laboratory, Upton, New York 11973
(Received 2 September 1981)

The total cross sections for $\nu_\mu n$ and $\nu_\mu p$ charged-current interactions and their ratio $R = \sigma_T(\nu n)/\sigma_T(\nu p)$ have been measured as a function of neutrino energy from 0.4 to 10 GeV. The experiment is performed using the BNL 7-foot deuterium bubble chamber exposed to the Alternating Gradient Synchrotron wide-band neutrino beam. The absolute values of the cross sections are normalized to the quasielastic scattering ($\nu_\mu n \rightarrow \mu^- p$) cross section. Above 1.6 GeV the data are consistent with the quark-parton model. We find that $\sigma_T(\nu n)/E_\nu = (1.07 \pm 0.05) \times 10^{-38}$, $\sigma_T(\nu p)/E_\nu = (0.54 \pm 0.04) \times 10^{-38}$, and $\sigma_T(\nu N)/E_\nu = (0.80 \pm 0.03) \times 10^{-38}$ cm²/GeV for $\langle E_\nu \rangle = 3.2$ GeV, and $R = 1.95 \pm 0.10$ for $\langle E_\nu \rangle = 3.7$ GeV.

I. INTRODUCTION

This paper reports the results of an experiment to measure the total cross sections for the $\nu_\mu n$ and $\nu_\mu p$ charged-current (CC) interactions, from 0.4 to 10 GeV. There have been numerous previous measurements of ν_μ -nucleon total cross sections $\sigma_T(\nu N)$ over a wide range of neutrino energies. However, all experiments suffered from differing systematic uncertainties in neutrino-flux calculations and the results have not always been consistent with each other.¹ The present experiment is performed using the BNL 7-foot bubble chamber exposed to the Alternating Gradient Synchrotron (AGS) wide-band neutrino beam. Details of the experimental arrangement have been published previously.² In this experiment the absolute values of the cross sections are normalized to the quasielastic scattering ($\nu n \rightarrow \mu^- p$) cross section using the known weak nucleon form factors. In the simple quark-parton model (QPM), the slope parameter $\sigma_T(\nu N)/E_\nu$ in the deep-inelastic region is independent of energy except for possible threshold effects due to charm production. With the presence of asymptotic freedom (ASF) of quantum chromo-

dynamics (QCD), $\sigma_T(\nu N)/E_\nu$ is expected to fall with increasing energy.³ However at high energies ($E_\nu \gtrsim 40$ GeV), the expected changes in $\sigma_T(\nu N)/E_\nu$ are very weak. Therefore, it is interesting to verify at what energy the QPM will start to describe our low-energy data, which are dominated by the quasielastic and $\Delta^{+,++}(1232)$ production channels, and to measure $\sigma_T(\nu N)/E_\nu$ as a function of energy. A detailed analysis of the cross-section ratio $R = \sigma_T(\nu n)/\sigma_T(\nu p)$ is also presented.

II. DATA ANALYSIS

A. The CC data sample

The data come from a total of 1 000 000 (200 000) pictures from the 7-foot bubble chamber filled with deuterium (hydrogen). The chamber was exposed to a wide-band neutrino beam with an average energy of 1.6 GeV. The film was scanned for neutral-induced interactions (≥ 2 prongs) in the chamber and approximately one-third of the film was rescanned. Each event was measured and processed through the TVGP kinematic program and

then reviewed by physicists to verify the results of the measurements, and to try to resolve ambiguous particle identification by means of ionization.

CC events are required to satisfy the following selection criteria:

- (i) The event has at least one negative particle which leaves the chamber or undergoes a μ^-e^- decay.
- (ii) The total visible momentum ($|\vec{P}_{\text{vis}}|$) is greater than $0.3 \text{ GeV}/c$ and the angle (θ_{vis}) between \vec{P}_{vis} and the beam direction is less than 50° . These criteria severely reduce the backgrounds due to incoming neutron or charge-particle interactions while cutting only 1% of the neutrino interactions.
- (iii) The neutrino interaction takes place inside a fiducial volume of 4 m^3 out of the 6 m^3 visible volume.
- (iv) The event has no constrained fits to an incoming charge-particle scatter hypothesis.
- (v) The event is kinematically consistent with being a neutrino interaction-i.e.,

$$C_{||} = E_{\text{vis}} - M_{\text{tgt}} - |\vec{P}_{\text{vis}}| \cos\theta_{\text{vis}} \\ \leq 160 \text{ (50) MeV in } D_2 \text{ (H}_2\text{)} .$$

This selection procedure yields 3723 (233) CC events in D_2 (H_2).

The $\bar{\nu}_\mu$ background in the CC sample is negligible in the present experiment. The main sources of background in the CC sample are neutral-current (NC) reactions and neutron-induced reactions where a π^- leaves the chamber without interacting. On the basis of the π^- detection efficiency (60%) and the observed number of NC candidates which have no possible μ^- track, we estimate this background to be $(6 \pm 1)\%$.

Since the neutrino-beam direction is known to within $\pm 0.5^\circ$, three-constraint (3C) kinematic fits have been made for all events to the following reactions:

$$vd \rightarrow \mu^- pp_s l (\pi^+ \pi^-), \quad l = 0, 1, \dots, \\ vd \rightarrow \mu^- p \pi^+ n_s l (\pi^+ \pi^-), \quad l = 0, 1, \dots,$$

where p_s and n_s are the spectator proton and neutron, respectively. If the spectator nucleon was not measurable, the standard bubble-chamber method was used for assigning an initial value of $(0 \pm 45) \text{ MeV}/c$ to the spectator momentum components.² 0C fits were also attempted for the unconstrained events assuming only single neutral particle, either n or π^0 depending on the presence or absence of an identified proton in the final states. For an appropriate fraction of 0C events, the average

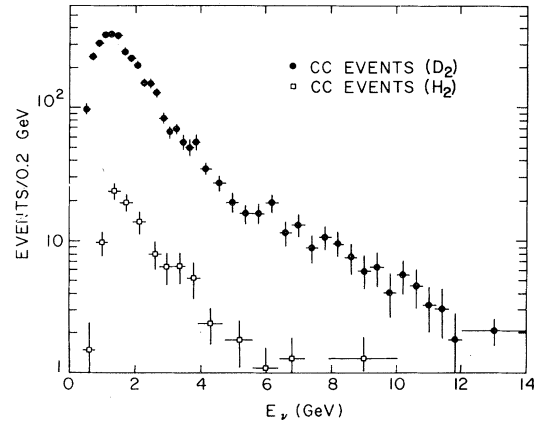


FIG. 1. Distributions of the observed neutrino energy E_ν for the selected CC events in D_2 and in H_2 .

$M(p\pi^-)$ or $M(\pi^+\pi^-)$ mass obtained from the 3C-fit multipion production events was imposed instead of the n or π^0 mass to correct the events with two neutral particles in the final states. Since the number of events fall rapidly as a function of track multiplicity, this treatment introduces little bias to the data. The constrained events were required to have at least one fit with a χ^2 probability $P(\chi^2) \geq 1\%$. In addition, the particle identification had to be consistent with the accepted final states.

The large chamber volume, the plates, the trapping power of the high magnetic field, and the relatively-low-energy neutrino beam made particle identification possible in a significant sample of the data. Kinematic fitting with particle identification allows us to select 2 115 (115) unique-3C-fit events and 913 (86) unique-0C-fit events from the D_2 (H_2) sample. Events with ambiguous final states are given appropriate weights based on χ^2 probabilities in the 3C cases and equal weights in the 0C cases, in all distributions. The average neutrino energy resolution $\Delta E_\nu/E_\nu$ is about 2 (5) % for the 3C-C-(0) fit events and does not distort seriously the final results of cross sections as a function of energy. The distribution of events in neutrino energy for the selected CC events is shown in Fig. 1.

B. Separation of νp interactions from νn interactions

An accurate separation of neutrino interactions on protons from those on neutrons in the deuteron target can be made on the basis of the total charge of charged particles (Q_t) and the number of visible

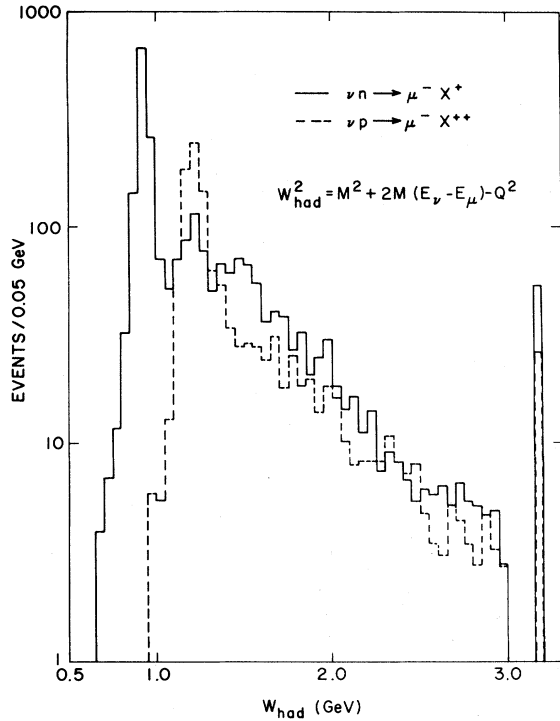


FIG. 2. Distributions of the effective mass of the hadronic system W_{had} for the νn and the νp events.

- (i) $Q_t=0$, $0 \leq P_v \leq 1$: $\nu n \rightarrow \mu^- X^+(p_s)$, where $P_s < 120 \text{ MeV}/c$;
- (ii) $Q_t=1$, $0 \leq P_v \leq 1$: $\nu p \rightarrow \mu^- X^{++}(n_s)$;
- (iii) $Q_t=1$, $P_v=2$: $\nu n \rightarrow \mu^- p X^0 P_s$, where $P_s \geq 120 \text{ MeV}/c$.

In order to estimate how many νp events are misclassified as νn events and vice versa by this separation method, we have investigated carefully various distributions of the H_2 sample and events with a visible spectator proton. The separation method applied to the D_2 sample was also applied to the H_2 sample. Only $(3 \pm 1)\%$ of the νp events were misclassified as νn events. The effect of rescattering, whereby the secondary particles from a ν -nucleon interaction interact with the spectator nucleon, may change the topology of a νn event to a νp event. Unfortunately there are no experimental data or reliable theoretical calculations on rescattering effects in the νd interactions. If one can attribute an excess of spectator protons at high momentum in the 3C-fit νn events, compared with the prediction of the Hulthén wave function, then the rescattering rate is 5%. The observed asymmetry between the forward and the backward spec-

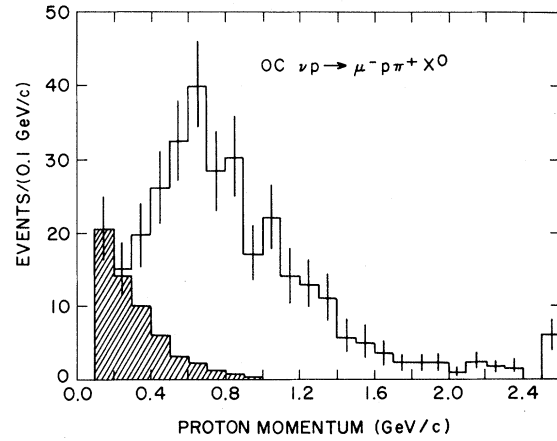


FIG. 3. Estimated νn contamination (shaded area) in the OC νp events.

protons (P_v) in the accepted final states. In this experiment protons with momentum greater than $\sim 120 \text{ MeV}/c$ are visible and measurable. Since most hadron tracks are slow ($p < 1 \text{ GeV}/c$) the use of ionization information and kinematic fitting enables one to uniquely identify almost all proton tracks. Each event can be classified as follows:

tator protons, with respect to the beam direction, also indicates the same rescattering rate. We have estimated possible rescattering effects more directly by comparing the proton momentum distributions in the OC νp events from the D_2 sample and from H_2 samples and found that $(5 \pm 1)\%$ of the νp events were actually νn events where the spectator proton was misidentified as the recoil proton. In this estimation we assumed that the spectator-proton momentum distribution (including rescattering) was universal for all channels. Figure 3 shows the estimate νn contamination in the OC νp events. A correlation for hydrogen contamination in the deuterium is applied for the νp events.

III. RESULTS

The distribution of events in neutrino energy for the 3C $\nu d \rightarrow \mu^- pp_s$ events is shown in Fig. 4 to-

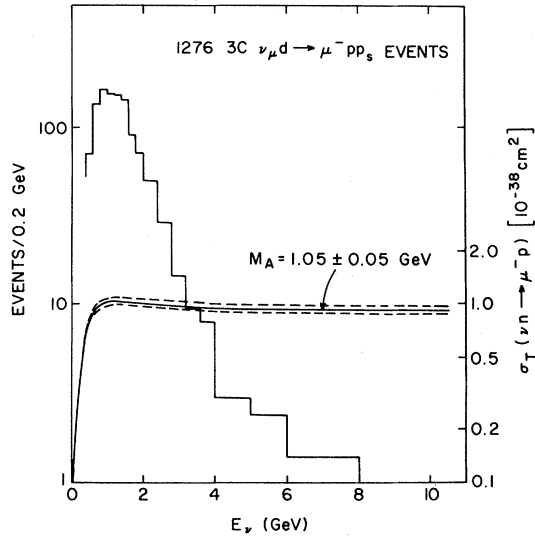


FIG. 4. The E_ν distribution for the $3C \nu d \rightarrow \mu^- pp_s$ events and the quasielastic cross section $\sigma(\nu n \rightarrow \mu^- p)$ calculated by the $V-A$ theory with $M_A = 1.05 \pm 0.05$ GeV.

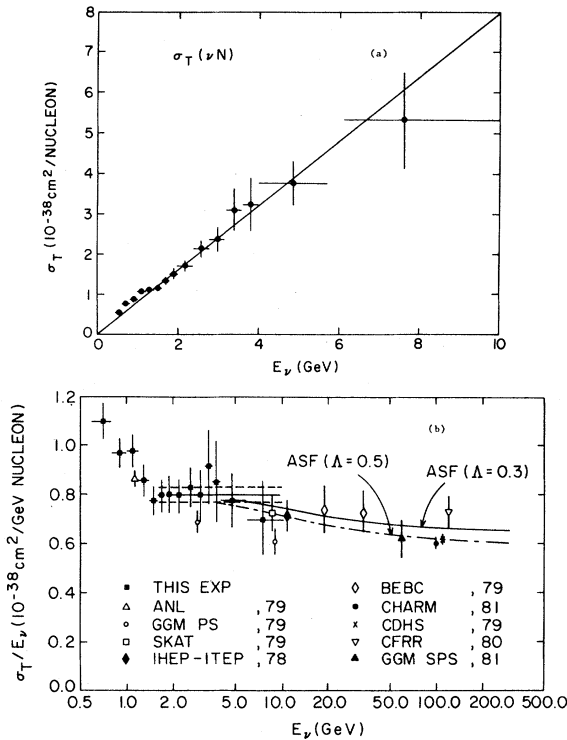


FIG. 5. (a) total cross section for the νN CC interactions $\sigma_T(\nu N)$ as a function of energy. The solid line is the best linear fit for $E_\nu > 1.6$ GeV; (b) comparison of the slope parameter $\langle \sigma_T(\nu N)/E_\nu \rangle$ for various experiments (Ref. 5). The curves are for the QPM with the leading order of asymptotic-freedom (ASF) effects for two values of Λ where Λ is the QCD parameter.

gether with the quasielastic cross section $\sigma(\nu n \rightarrow \mu^- p)$ calculated using the standard $V-A$ theory with $M_A = 1.05 \pm 0.05$ GeV and $M_V = 0.84$ GeV. The absolute cross sections for the CC interactions have been measured using the quasielastic events and its known cross section.⁴ The resulting nucleon total cross section $\sigma_T(\nu N) = \frac{1}{2}[\sigma_T(\nu n) + \sigma_T(\nu p)]$, is plotted as a function of energy up to 10 GeV in Fig. 5(a). The errors shown in the figure include both statistical and systematic errors. Above 3 GeV the statistical errors dominate because of the limited number of quasielastic events. It is clear that above ~ 1.5 GeV the total cross section rises linearly. Using only events with $E_\nu > 1.6$ GeV, a linear fit yields

$$\sigma_T(\nu N) = [(0.02 \pm 0.23) + (0.80 \pm 0.11)E_\nu]$$

$$\times 10^{-38} \text{ cm}^2/\text{GeV/nucleon}$$

with $\chi^2/\text{DOF} = 1.27/7$ and $\langle E_\nu \rangle = 3.2$ GeV. Forcing $\sigma_T(\nu N) = 0$ at $E_\nu = 0$, a one-parameter fit yields

$$\sigma_T(\nu N) = (0.80 \pm 0.03)E_\nu$$

with $\chi^2/\text{DOF} = 1.28/8$.

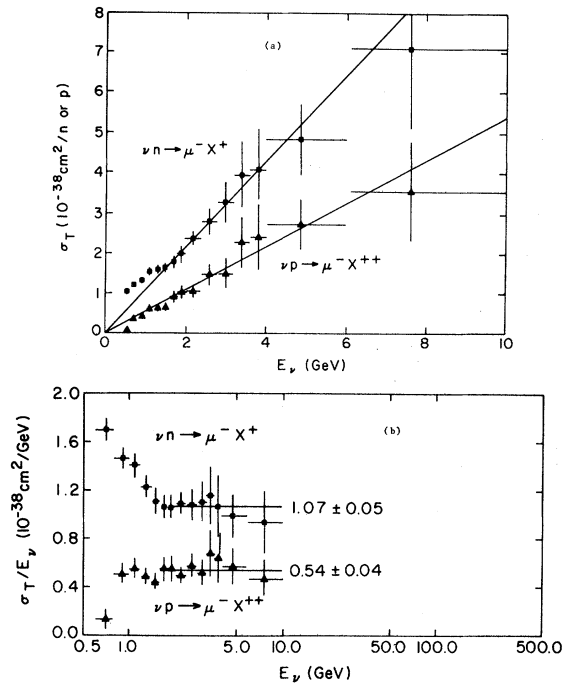


FIG. 6. (a) total cross section for νn and νp interactions as a function of energy; (b) the slope parameters $\sigma_T(\nu n)/E_\nu$ and $\sigma_T(\nu p)/E_\nu$ as a function of energy. The solid lines are the best fits for $E_\nu > 1.6$ GeV.

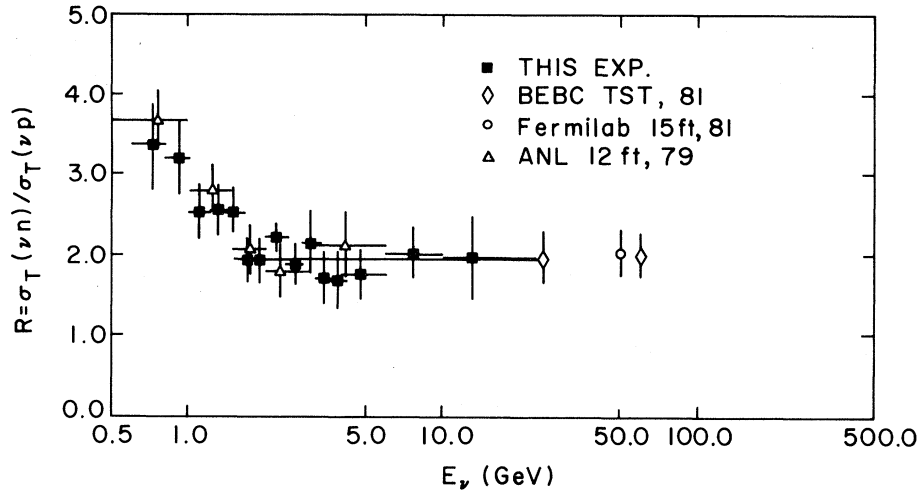


FIG. 7. The cross-section ratio $R = \sigma_T(\nu n) / \sigma_T(\nu p)$ as a function of energy. (TST stands for track-sensitive target.) The solid line is the weighted average from 1.6 to 24 GeV.

For $E_\nu > 1.6$ GeV the data are consistent with the energy independence of the slope parameter $\sigma_T(\nu N) / E_\nu$ within the experimental errors. Our value is $\sim 30\%$ higher than the current (1980) world average of $\sigma_T(\nu N) / E_\nu = 0.63 \pm 0.02$ which is dominated by high-energy experiments.¹ Figure 5(b) shows $\sigma_T(\nu N) / E_\nu$ versus E_ν together with recent published results.⁵ Compared with the high-energy data ($E_\nu \geq 50$ GeV) it appears that $\sigma_T(\nu N) / E_\nu$ is not independent of energy but rather falls slowly as neutrino energy increases. This trend is consistent with the expectations for the leading-order calculation of QCD (ASF) as shown

in Fig. 5(b).

The total cross sections for the νn and the νp interactions and the slope parameters $\nu_T(\nu n) / E_\nu$ and $\nu_T(\nu p) / E_\nu$ are shown in Figs. 6(a) and (b). Again, for $E_\nu > 1.6$ GeV both slope parameters are independent of energy within the errors and linear fits give

$$\sigma_T(\nu n) = (1.07 \pm 0.05) E_\nu \times 10^{-38} \text{ cm}^2 / \text{GeV}$$

with $\chi^2 / \text{DOF} = 0.8 / 8$ and

$$\sigma_T(\nu p) = (0.54 \pm 0.04) E_\nu \times 10^{-38} \text{ cm}^2 / \text{GeV}$$

with $\chi^2 / \text{DOF} = 1.6 / 8$. Therefore the data are sup-

TABLE I. Comparison of recent measurements of the cross-section ratio $R = \sigma_T(\nu n) / \sigma_T(\nu p)$

Experiment	E_ν ($\langle E_\nu \rangle$) (GeV)	R	Cuts
ANL 12 ft (Ref. 5)	1.5–6.0	1.95 ± 0.21	None
GGM PS (Ref. 6)	1.0–10.0	2.08 ± 0.15	None
Fermilab 15 ft (Ref. 7)	10–200 (50)	2.03 ± 0.28	$W_{\text{had}} > 1.5$ GeV
BEBC TST (Ref. 8)	(25), (60)	1.98 ± 0.19	None
This experiment (A)	1.6–24.0 (3.7)	1.95 ± 0.10	None
(B)		1.82 ± 0.13	$W_{\text{had}} > 1.4$ GeV
(C)		1.79 ± 0.15	$W_{\text{had}} > 1.4$ GeV and $Q^2 > 0.7$ (GeV/c) ²
QPM (Ref. 9) (A)		1.95	Excluding s -quark contributions
(B)		1.88	Including s -quark contributions

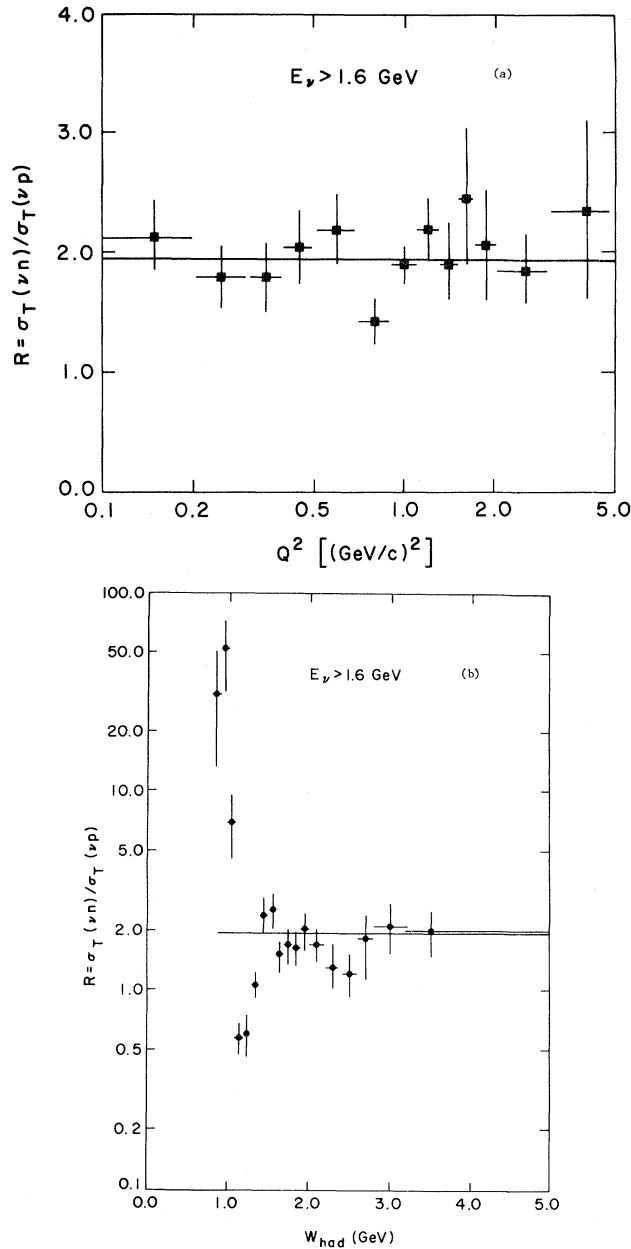


FIG. 8. (a) R as a function of Q^2 and (b) R as a function of W_{had} for $E_\nu > 1.6$ GeV. The solid lines are the weighted average.

porting the conjecture of scaling and of a pointlike substructure in the neutron and the proton.

The relative cross-section ratios $R = \sigma_T(\nu n) / \sigma_T(\nu p)$ are plotted as a function of energy in Fig. 7. In the determination of R the errors are free from the uncertainty in the quasielastic cross section ($\pm 5\%$). In the energy range from 0.4 to 1.5

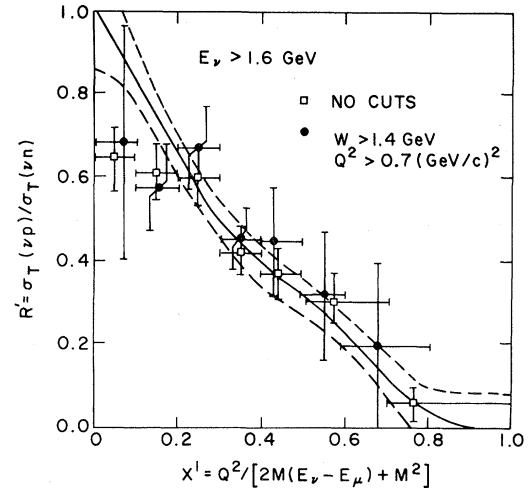


FIG. 9. $R' = 1/R$ as a function of $x' = Q^2 / [2M(E_\nu - E_\mu) + M^2]$ without and with a deep inelastic cut [$W_{\text{had}} > 1.4$ GeV and $Q^2 > 0.7$ (GeV/c) 2]. The curves are the QPM predictions of Ref. 10.

GeV the value of R falls and then approaches an asymptotic value of approximately 2. By integrating the events from 1.6 to 24 GeV, we measure

$$R = 1.95 \pm 0.10$$

for $\langle E_\nu \rangle = 3.7$ GeV, $\langle Q^2 \rangle = 1.0$ (GeV/c) 2 and $\langle W_{\text{had}} \rangle = 1.6$ GeV. This value is in good agreement with the QPM and with other recent experiments⁵⁻⁸ even though the beam energies and experimental cuts differ between experiments as summarized in Table I. In the QPM, R is related to the x distributions of up, down, and strange quarks and antiquarks defined in the proton

$$R = \frac{\int x[u(x) + s(x) + \bar{d}(x)]/3 dx}{\int x[d(x) + s(x) + \bar{u}(x)]/3 dx},$$

where $x = Q^2 / [2M(E_\nu - E_\mu)]$. This is of the order of 2 if only the three valence quarks contribute. Using the scaling quark structure function deduced from electroproduction data, the QPM predicts a value of ~ 1.88 including the s -quark contributions.⁹ If the s -quark contributions are excluded, then it predicts a value of ~ 1.95 . In principle the model only works for deep-inelastic interactions which are usually defined as interactions with $W_{\text{had}} > 2$ GeV and $Q^2 > 1$ GeV $^2/c^2$. However, our data consist mainly of quasielastic and one-pion interactions. Therefore in Fig. 8(a) we show $R(E > 1.6$ GeV) as a function of Q^2 and in Fig. 8(b) as a function of W_{had} . One can easily see that R is

independent of Q^2 but oscillates strongly with W_{had} due to the presence of the quasielastic reaction, Δ and N^* resonances. However, if one averages R over the appropriate W_{had} region, the scaling seems to persist even in the low- W_{had} region. A more sensitive test of scaling can be done by plotting R as a function of the scaling variable $x' = Q^2/[2M(E_\nu - E_\mu) + M^2]$ and comparing it to the QPM prediction using $R_e(x') = \sigma_T(en)/\sigma_T(ep)$ from electroproduction data.¹⁰ Figure 9 shows $R' = 1/R = \sigma_T(vp)/\sigma_T(vn)$ without cuts and R' with $W_{\text{had}} > 1.4$ GeV and $Q^2 > 0.7$ (GeV/c)². It can be seen that the QPM prediction is in agreement with the data both with and without cuts. At high x' ($\gtrsim 0.3$), where the sea-quark contributions are expected to be small and $R' \sim d(x')/u(x')$, the majority (u) quarks seem to dominate over the minority (d) quark in the proton. Results from high-energy experiments also show the same tendency.^{7,8}

IV. CONCLUSIONS

We have measured the total cross section for the $\nu_{\mu}N$ CC interactions in the energy range 0.4–10 GeV which is free from systematic uncertainties in neutrino-flux calculations. The value of $\sigma_T(\nu N)/E_\nu$ falls significantly from 0.4 to 1.5 GeV

and then becomes constant. Above $E_\nu > 1.6$ GeV we find $\sigma_T(\nu N)/E_\nu = (0.80 \pm 0.03) \times 10^{-38}$ cm²/GeV/nucleon for $\langle E_\nu \rangle = 3.2$ GeV, which is $\sim 30\%$ higher than the 1980 world average of $\sigma_T(\nu N)/E_\nu = 0.63 \pm 0.02$. However, taken in conjunction with the recent high-energy results, it is clear that $\sigma_T(\nu N)/E_\nu$ decreases with increasing energy. This trend of the data is consistent with the expectations of the QPM with the leading order of asymptotic-freedom effects. We have also measured the total cross sections for the $\nu_{\mu}n$ and the $\nu_{\mu}p$ CC interactions separately, and their ratio $R = 1.95 \pm 0.10$. Although our data are in the resonance region, averaging our data above 1.6 GeV, the results are consistent with the QPM predictions.

ACKNOWLEDGMENTS

We wish to express our thanks to the staffs of the AGS and the 7-foot bubble chamber who made this experiment possible. We also would like to thank our scanning-measuring personnel at BNL for their painstaking efforts. This work is supported by the U.S. Department of Energy under Contract No. DE-AC02-76CH00016.

¹Particle Data Group, Rev. Mod. Phys. **52**, S54 (1980).

²N. J. Baker *et al.*, Phys. Rev. D **23**, 2499 (1981); N. J. Baker *et al.*, *ibid.*, **23**, 2495 (1981).

³A. J. Buras, Rev. Mod. Phys. **52**, 199 (1980); A. J. Buras and K. J. F. Gamers, Phys. Lett. **71B**, 106 (1977).

⁴If one increases the value of M_A by 5%, then one should also increase the absolute cross sections by 5%.

⁵S. J. Barish *et al.*, Phys. Rev. D **19**, 2521 (1979) [ANL]; S. Clampolillo *et al.*, Phys. Lett. **84B**, 281 (1979) [Gargamelle, CERN Proton Synchrotron (GGM PS)]; D. S. Baranov *et al.*, *ibid.*, 255 (1979) [SKAT]; A. E. Asratyan *et al.*, *ibid.*, **76B**, 239 (1978) [IHEP-ITEP]; D. C. Colley *et al.*, Z. Phys. C **2**, 187 (1979) [BEBC]; M. Jonker *et al.*, Phys. Lett. **99B**,

265 (1981) [CHARM]; J. G. H. de Groot *et al.*, Z. Phys. C **1**, 143 (1979) [CERN-Dortmund-Heidelberg-Saclay (CDHS)]; B. Barish *et al.*, in *High Energy, Physics—1980*, proceedings of the XX International Conference, Madison, Wisconsin, 1980, edited by L. Durand and L. G. Pondrom (AIP, New York 1981) p. 741 [Caltech-Fermilab-Rochester-Rockefeller (CFRR)]; J. Morfin *et al.*, Phys. Lett. **104B**, 235 (1981) [GGM SPS]; C. Baltay *et al.*, Phys. Rev. Lett. **44**, 916 (1980) [not shown in Fig. 5(b)].

⁶W. Lerche *et al.*, Nucl. Phys. **B142**, 65 (1978).

⁷J. Hanlon *et al.*, Phys. Rev. Lett. **45**, 1817 (1980).

⁸N. Armenise *et al.*, Phys. Lett. **102B**, 374 (1981).

⁹R. D. Field and R. P. Feynman, Phys. Rev. D **15**, 2590 (1977).

¹⁰A. Bodek *et al.*, Phys. Rev. D **20**, 1471 (1979).